PHYSICAL REVIEW D **95,** 043513 (2017)

Testing coupled dark energy models with their cosmological background evolution

Carsten van de Bruck,[*] Jurgen Mifsud,[†] and Jack Morrice[‡]

Consortium for Fundamental Physics, School of Mathematics and Statistics, University of Sheffield, Hounsfield Road, Sheffield S3 7RH, United Kingdom

(Received 24 October 2016; published 16 February 2017)

We consider a cosmology in which dark matter and a quintessence scalar field responsible for the acceleration of the Universe are allowed to interact. Allowing for both conformal and disformal couplings, we perform a global analysis of the constraints on our model using Hubble parameter measurements, baryon acoustic oscillation distance measurements, and a Supernovae Type Ia data set. We find that the additional disformal coupling relaxes the conformal coupling constraints. Moreover, we show that, at the background level, a disformal interaction within the dark sector is preferred to both ΛCDM and uncoupled quintessence, hence favoring interacting dark energy.

DOI: 10.1103/PhysRevD.95.043513

I. INTRODUCTION

Multiple high precision cosmological observations broaden our understanding of the dynamics of the Universe when confronted with theoretical models. For instance, inferences from observations of Supernovae Type Ia (SNIa) [1–5], baryon acoustic oscillations (BAO) [6–8], and the cosmic microwave background (CMB) [9–12] are complementary—among other things, they indicate that our Universe has recently entered an accelerating epoch. Analysis from data sets of this kind has led cosmologists to formulate a standard model that postulates a dark sector consisting of dark energy and dark matter, contributing to about 69% and 26% of the total energy density in the Universe, respectively [12]. The focus of much current research in cosmology is to understand the properties and origins of the dark sector, in particular dark energy, for which the cosmological constant is the simplest explanation [13]; this standard model is currently in very good agreement with current cosmological observations. Theoretically, however, the coincidence and fine-tuning problems challenge our understanding of gravity and quantum field theory [14,15]. A plethora of alternative dynamical dark energy models have been proposed, such as quintessence [16–18], k-essence [19,20], phantom [21], Chaplygin gas [22], Ricci dark energy [23], and holographic dark energy and related ideas [24,25]. Furthermore, coupled dark energy models have also been extensively studied since, from the field theoretic point of view, dark energy is not prohibited from interacting with cold dark matter [26–39] or, for example, massive neutrinos [40–44].

In this paper, we consider the case of a (nonuniversally) coupled dark energy model in which dark matter particles feel an additional fifth force mediated by the dark energy scalar field. This coupling between the dark sector elements modifies the background evolution of the Universe, as well as the growth of perturbations; in this paper, we concentrate on constraints coming from the background only, deferring the perturbed case for future work. As conformally coupled dark matter models have been well studied [45–53], and tight constraints on the model parameters have been established [50–52], the main aim of this paper is to augment the models of these studies with a disformal coupling and discern its influence in light of the conformal-only constraints. Models that utilize such disformal interactions within the dark sector have been attracting much attention recently [33,38,54–61], so it has become imperative that they be compared with state-of-the-art cosmological data sets.

This paper is structured as follows. In Sec. II, we introduce our coupled dark energy model and present the background evolution equations in a flat, homogeneous, and isotropic Universe. We list in Sec. III the observational data sets we will use here to derive constraints on our model parameters, while in Sec. IV, we present the obtained constraints for each coupled dark matter model. Finally Sec. V contains our conclusions and outlines future work.

II. THEORETICAL MODEL: ACTION AND EQUATIONS OF MOTION

We consider the scalar-tensor theory described by the following action, expressed in the Einstein frame,

$$\mathcal{S} = \int d^4x\sqrt{-g}\left[\frac{M_{\rm Pl}^2}{2}R - \frac{1}{2}g^{\mu\nu}\partial_\mu\phi\partial_\nu\phi - V(\phi) + \mathcal{L}_{\rm SM}\right] + \int d^4x\sqrt{-\tilde{g}}\tilde{\mathcal{L}}_{\rm DM}(\tilde{g}_{\mu\nu},\psi), \tag{1}$$

where $\kappa^2 \equiv M_{\rm Pl}^{-2} \equiv 8\pi G$ such that $M_{\rm Pl} = 2.4 \times 10^{18}$ GeV is the reduced Planck mass; dark energy is described by a

[*]c.vandebruck@sheffield.ac.uk
[†]jmifsud1@sheffield.ac.uk
[‡]app12jam@sheffield.ac.uk

quintessence scalar field, ϕ, with a potential, $V(\phi)$; and the uncoupled standard model (SM) particles are described by the Lagrangian, $\mathcal{L}_{\rm SM}$, which includes a relativistic component, r, and a baryon component, b. Particle quanta of the dark matter (DM) fields, ψ, propagate on geodesics defined by the metric

$$\tilde{g}_{\mu\nu} = C(\phi)g_{\mu\nu} + D(\phi)\partial_\mu\phi\partial_\nu\phi, \tag{2}$$

with $C(\phi)$ and $D(\phi)$ being the conformal and disformal coupling functions, respectively. In the general case, the free functions C and D can depend on the kinetic term $X = -\frac{1}{2}g^{\mu\nu}\partial_\mu\phi\partial_\nu\phi$ as well, but throughout this paper, we will not consider such a scenario. By definition, in the Einstein frame, the gravitational sector has the Einstein–Hilbert form, and SM particles are not coupled to the scalar field directly.

The action above defines an interaction between DM and dark energy, resulting from the modification of the gravitational field experienced by the DM particles, $\tilde{g}_{\mu\nu}$, by the dark energy scalar field.

Variation of the action (1) with respect to the metric $g_{\mu\nu}$ leads to the field equations

$$R_{\mu\nu} - \frac{1}{2}g_{\mu\nu}R = \kappa^2(T^\phi_{\mu\nu} + T^{\rm SM}_{\mu\nu} + T^{\rm DM}_{\mu\nu}), \tag{3}$$

where the energy-momentum tensors of the scalar field, SM particles, and DM particles are defined by

$$T^\phi_{\mu\nu} = \partial_\mu\phi\partial_\nu\phi - g_{\mu\nu}\left(\frac{1}{2}g^{\rho\sigma}\partial_\rho\phi\partial_\sigma\phi + V(\phi)\right),$$

$$T^{\rm SM}_{\mu\nu} = -\frac{2}{\sqrt{-g}}\frac{\delta(\sqrt{-g}\mathcal{L}_{\rm SM})}{\delta g^{\mu\nu}}, \quad T^{\rm DM}_{\mu\nu} = -\frac{2}{\sqrt{-g}}\frac{\delta(\sqrt{-\tilde{g}}\tilde{\mathcal{L}}_{\rm DM})}{\delta g^{\mu\nu}},$$

respectively. Nonconservation of $T^\phi_{\mu\nu}$ implies the following relation,

$$\Box\phi = V_{,\phi} - Q, \tag{4}$$

where

$$Q = \frac{C_{,\phi}}{2C}T_{\rm DM} + \frac{D_{,\phi}}{2C}T^{\mu\nu}_{\rm DM}\nabla_\mu\phi\nabla_\nu\phi - \nabla_\mu\left[\frac{D}{C}T^{\mu\nu}_{\rm DM}\nabla_\nu\phi\right], \tag{5}$$

and $T_{\rm DM}$ is the trace of $T^{\mu\nu}_{\rm DM}$, which satisfies a modified conservation equation

$$\nabla^\mu T^{\rm DM}_{\mu\nu} = Q\nabla_\nu\phi. \tag{6}$$

Since SM particles are uncoupled from the scalar field, their energy-momentum tensor obeys the standard conservation equation

$$\nabla^\mu T^{\rm SM}_{\mu\nu} = 0. \tag{7}$$

We assume all species to be perfect fluids,

$$T^{\mu\nu}_i = (\rho_i + p_i)u^\mu u^\nu + p_i g^{\mu\nu}, \tag{8}$$

where the index i stands for DM and SM. The Einstein frame SM and DM fluid's energy density and pressure are denoted by ρ_i and p_i, respectively.

As we stated in the Introduction, only the background dynamics of the theory are considered in this work—a study of the perturbations will appear in a future publication, and so, from now on, we will consider the standard flat Friedmann-Robertson-Walker metric, given by

$$ds^2 = g_{\mu\nu}dx^\mu dx^\nu = a^2(\tau)[-d\tau^2 + \delta_{ij}dx^i dx^j], \tag{9}$$

with conformal time τ, we will denote a conformal time derivative by a prime and scale factor $a(\tau)$. Spatial gradients in the scalar field, ϕ, and matter fluid variables, ρ_i and p_i, are hence also neglected for this first paper.

Given the above simplifications, the modified Klein-Gordon equation (4) becomes

$$\phi'' + 2\mathcal{H}\phi' + a^2V_{,\phi} = a^2Q; \tag{10}$$

the fluid conservation equations simplify to

$$\rho_r' + 4\mathcal{H}\rho_r = 0, \tag{11}$$

$$\rho_b' + 3\mathcal{H}\rho_b = 0, \tag{12}$$

$$\rho_c' + 3\mathcal{H}\rho_c = -Q\phi'; \tag{13}$$

and the Friedmann equations simplify to

$$\mathcal{H}^2 = \frac{\kappa^2}{3}a^2(\rho_\phi + \rho_b + \rho_r + \rho_c), \tag{14}$$

$$\mathcal{H}' = -\frac{\kappa^2}{6}a^2(\rho_\phi + 3p_\phi + \rho_b + 2\rho_r + \rho_c), \tag{15}$$

where we now denote coupled DM by a subscript, c. The scalar field's energy density and pressure, respectively, have the usual forms $\rho_\phi = \phi'^2/(2a^2) + V(\phi)$ and $p_\phi = \rho_\phi - 2V(\phi)$, and we denote the conformal Hubble parameter by $\mathcal{H} = a'/a$. The coupling, as defined by Eq. (5), simplifies to [58]

$$Q = -\frac{a^2C_{,\phi} + D_{,\phi}\phi'^2 - 2D\left(\frac{C_{,\phi}}{C}\phi'^2 + a^2V_{,\phi} + 3\mathcal{H}\phi'\right)}{2\left[a^2C + D(a^2\rho_c - \phi'^2)\right]}\rho_c. \tag{16}$$

Throughout this paper, we choose an exponential scalar field potential,

$$V(\phi) = V_0^4 e^{-\lambda\kappa\phi}, \tag{17}$$

where V_0 and λ are constants. When we consider a conformal coupling, we make use of an exponential function,

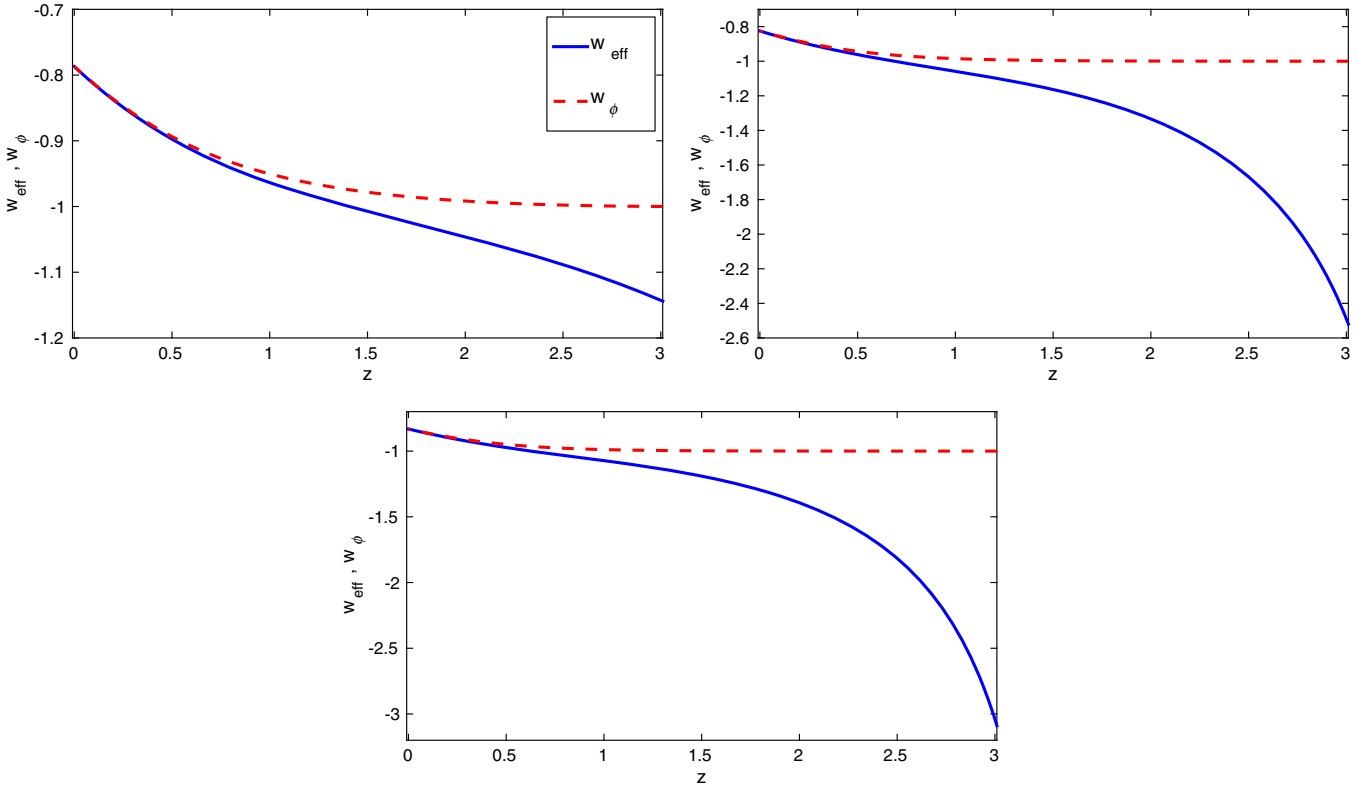

FIG. 1. These figures show the evolution of the effective equation of state (solid) and the corresponding evolution of the scalar field equation of state parameter (dashed). We show a conformal case with $\alpha = 0.02$ (left), a disformal case with $D_M = 0.34$ meV^{-1} (right), and a conformal disformal case with $\alpha = 0.02$ and $D_M = 0.34$ meV^{-1} (bottom). In all cases, we set $\lambda = 1.2$.

$$C(\phi) = e^{2\alpha\kappa\phi}, \tag{18}$$

where α is a constant. As this is a simple first study, we only take into account a constant disformal coupling,

$$D(\phi) = D_M^4, \tag{19}$$

where D_M is a constant inverse mass scale, expressed in meV^{-1}.

Let us now consider a phenomenological reparametrization of the system made concrete above. We will find interpretation of our parameter constraints in the following sections is made much more clear if we reparametrize the system described above in the following way, and we will return to comment on these definitions with regard to our results in later sections. Following Refs. [38,60,62,63], we repackage the dark sector of our model by now defining an effective dark energy fluid, $\rho_{\rm DE,eff}$, with effective equation of state, $w_{\rm eff}(z)$, such that

$$\rho'_{\rm DE,eff} + 3\mathcal{H}(1 + w_{\rm eff})\rho_{\rm DE,eff} = 0, \tag{20}$$

and

$$\rho'_{\rm c,eff} + 3\mathcal{H}\rho_{\rm c,eff} = 0, \tag{21}$$

and hence

$$\mathcal{H}^2 = \frac{\kappa^2}{3} a^2(\rho_{\rm DE,eff} + \rho_b + \rho_r + \rho_{c,0}a^{-3}). \tag{22}$$

In this reparametrized system, there are by definition no dark sector interactions, and the DM energy density dilutes with the expansion as a^{-3}. By comparing these noninteracting dark sector definitions with our coupled dark energy model equations, we get that

$$w_{\rm eff} = \frac{p_\phi}{\rho_{\rm DE,eff}} = \frac{p_\phi}{\rho_\phi + \rho_c - \rho_{c,0}a^{-3}}. \tag{23}$$

Since the coupled DM energy density does not redshift as a^{-3}, it follows that, although $w_\phi \in [-1, 1]$, $w_{\rm eff}$ can take values less than -1. We have defined $w_{\rm eff}$ in Eq. (23) above such that, evaluated today, the effective equation of state coincides with the scalar field equation of state parameter. We illustrate the evolution of the effective equation of state and the scalar field equation of state parameter in Fig. 1 for three different coupling scenarios.

III. OBSERVATIONAL DATA SETS

For our main analysis presented in Sec. IV, we shall be considering constraints on the cosmological parameters derived from the late-time Universe expansion history. We shall be considering Hubble parameter measurements [64]

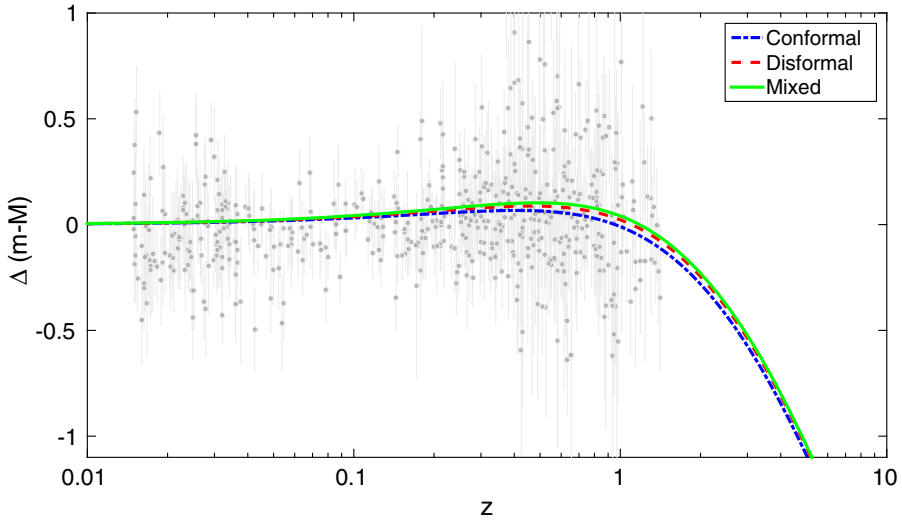

FIG. 2. In this figure, we show the distance modulus for three different models together with the supernova Union2.1 data set [68]. We illustrate a conformal case with $\alpha = 0.02$, a disformal case with $D_M = 0.4\ \mathrm{meV}^{-1}$, and a mixed conformal disformal case with $\alpha = 0.18$ and $D_M = 0.4\ \mathrm{meV}^{-1}$. In all cases, we set $\lambda = 1.1$.

and BAO data [65–67], together with SNIa data from the Union2.1 catalog [68]. Moreover, we shall be considering a standard big bang nucleosynthesis (BBN) prior corresponding to a baryon density $100\Omega_b h^2 = 2.202 \pm 0.046$ [69].

A. $H(z)$ data set and the Hubble constant

We use $H(z)$ data inferred from the differential age technique [70], a technique based on measurements of the age difference between two passively evolving galaxies that formed at the same time but are separated by a small redshift interval, i.e. a measurement of the derivative dz/dt, where t is the cosmic time and $H = a^{-1}\mathcal{H}$. In Sec. IV, we use 28 independent $H(z)$ measurements [64], between redshifts $0.07 \leq z \leq 2.3$, to place constraints on our model parameters. We also consider a Gaussian prior on the Hubble constant,[1] given by the Hubble Space Telescope measurement of $H_0 = 73.8 \pm 2.4\ \mathrm{km\,s^{-1}\,Mpc^{-1}}$ [72].

B. Baryon acoustic oscillations

BAO features in the clustering of galaxies are being used by large scale surveys as a standard ruler to measure the distance-redshift relation. The acoustic oscillations in the photon-baryon plasma arise from the tight coupling of baryons and photons in the radiation era. BAO data are usually reported in terms of the angle-averaged distance

$$D_V(z) = [z(1+z)^2 D_A^2(z) H^{-1}(z)]^{1/3}, \tag{24}$$

consisting of the angular diameter distance, $D_A(z)$, and the Hubble parameter. In the main analysis of Sec. IV, we use the CMASS and LOWZ samples from Data Release 12 of the Baryon Oscillation Spectroscopic Survey at $z_{\mathrm{eff}} = 0.57$ and $z_{\mathrm{eff}} = 0.32$, respectively [65]; the 6dF Galaxy Survey measurement at $z_{\mathrm{eff}} = 0.106$ [66]; and the Main Galaxy Sample of Data Release 7 of Sloan Digital Sky Survey at $z_{\mathrm{eff}} = 0.15$ [67].

C. Supernovae Type Ia

Apart from providing observational evidence for the accelerating expansion of the Universe [1–5], SNIa observations have also been widely used for cosmological model parameter fitting. In our analysis, we use the supernova Union2.1 compilation of 580 data points [68]. In Fig. 2, we show the residual Hubble diagram from an empty Universe, for three classes of models compared to the data set of Ref. [68]. The distance modulus is defined as [73]

$$\Delta(m-M) = (m-M)_{\mathrm{model}} - (m-M)_{\mathrm{Milne}},$$
$$m - M = 5\log_{10}\frac{D_L(z)}{10\ \mathrm{pc}}, \tag{25}$$

where m is the apparent magnitude, M is the absolute magnitude of the object, and $D_L(z)$ is the luminosity distance.

IV. PARAMETER CONSTRAINTS AND BEST FIT VALUES

For the global fitting of the cosmological parameters, we use a modified version of the CLASS code [74] to evolve the coupled dark energy-dark matter background equations, and interface with the public (Metropolis-Hastings) Markov chain Monte Carlo code Monte Python [75] to constrain the model parameter space with cosmological

[1]We are aware of a more recent measurement of the Hubble constant as reported in Ref. [71], although we decided to use a more conservative constraint in our analysis.

TABLE I. For each model parameter, we report the best fit values and 1σ errors in the conformally coupled DM scenario. For λ and α, we quote the 95.4% upper limits instead. See the top of Sec. IV for our chosen parameter priors. In the H_0 run, we further include the best fit value and 1σ errors for the conformal coupling strength parameter.

Parameter	$H(z)+\mathrm{BAO}+\mathrm{SNIa}$	$H(z)+\mathrm{BAO}+\mathrm{SNIa}+\mathrm{BBN}$	$H(z)+\mathrm{BAO}+\mathrm{SNIa}+\mathrm{BBN}+H_0$
$\Omega_b h^2$	$0.021^{+0.0072}_{-0.0069}$	$0.022^{+0.0005}_{-0.0005}$	$0.022^{+0.0005}_{-0.0005}$
$\Omega_c h^2$	$0.11^{+0.013}_{-0.011}$	$0.11^{+0.007}_{-0.007}$	$0.11^{+0.008}_{-0.008}$
H_0	$67.49^{+2.14}_{-2.18}$	$67.92^{+1.47}_{-1.57}$	$70.14^{+1.35}_{-1.63}$
λ	<1.27	<1.21	<1.05
α	<0.193	<0.143	$0.097^{+0.056}_{-0.039}(<0.168)$

data. The amplitude of the scalar field exponential potential function, V_0, is determined by using an iterative routine in the modified CLASS code. We assume top-hat priors for our parameters: the baryon energy density parameter $\Omega_b h^2 \in [0.005, 0.1]$, the coupled cold dark matter energy density parameter $\Omega_c h^2 \in [0.01, 0.99]$, the Hubble constant parameter $H_0 \in [45, 90]$ km s^{-1} Mpc^{-1}, the conformal coupling parameter $\alpha \in [0, 0.48]$, the disformal coupling parameter $D_M \in [0, 1.1]$ meV^{-1}, and the scalar field potential exponent parameter $\lambda \in [0, 1.7]$. We have chosen the range for our model parameters α, D_M, and λ to accommodate all the values for which there is acceleration at the present (see Ref. [61] for details). On top of these, we also include Gaussian priors on $\Omega_b h^2$ and H_0, as mentioned in Secs. III and III A, respectively. Hence, the most general parameter space in our analyses is given by $\Theta = \{\Omega_b h^2, \Omega_c h^2, H_0, \alpha, D_M, \lambda\}$.

Although in this paper we shall only consider positive values for our parameters, we have repeated the analyses presented below for a negative range of priors, and the obtained results were consistent with those presented here. Changing the scalar field's initial value, ϕ_{ini}, is equivalent to changing the field potential height parameter V_0, so we have held ϕ_{ini} fixed for the entire study.

A. Conformal case

We first discuss the well-known case in which DM is only conformally coupled [45–53]. Although already well documented, this case is presented here both as a consistency check and to provide the means to cleanly compare parameter constraints derived from the purely conformal case with the mixed case discussed in Sec. IV C. Our results from different runs of Monte Python are illustrated in Table I. The confidence-level contours and the corresponding one-dimensional posterior distributions for the $H(z)+\mathrm{BAO}+\mathrm{SNIa}$ (red contours) run, the $H(z)+\mathrm{BAO}+\mathrm{SNIa}+\mathrm{BBN}$ (blue contours) run, and the $H(z)+\mathrm{BAO}+\mathrm{SNIa}+\mathrm{BBN}+H_0$ (green contours) run are shown in Fig. 3. In Fig. 3, we show all covariance combinations, although for the two cases discussed below, we only show the most interesting combinations (which only involve the model parameters), since the obtained constraints in these models are weaker than those reported in the conformal case. Using the $H(z)+\mathrm{BAO}+\mathrm{SNIa}$ observations, we obtain an upper limit on the interaction coupling strength $\alpha < 0.193$ at the 95.4% C.L.

When we include the BBN prior on the baryon energy density parameter, the upper limit on the conformal coupling parameter improves slightly to $\alpha < 0.143$ at the 95.4% C.L., which is mainly due to better constraints on the cosmological parameters. The obtained upper limit is consistent with other results in the literature [45–52]. When using the H_0 prior in combination with the other data sets, the conformal coupling strength parameter upper limit increases, as expected [47,50,51], to $\alpha < 0.168$ (95.4% C.L.). Indeed, we find that the best fit value for the conformal coupling strength is away from zero at 1σ, $\alpha = 0.097^{+0.056}_{-0.039}$, but is consistent with zero at 2σ. This occurs mainly due to a slight tension between different values of H_0 deduced from the data sets. In this model, the potential slope λ is constrained to be $\lambda < 1.21$ (95.4% C.L.) without the H_0 prior, and $\lambda < 1.05$ (95.4% C.L.) when including the H_0 prior; both are consistent with results in the literature [46,49]. The data we use in our analysis is not able to tightly constrain the conformal coupling interaction parameter very well; tighter constraints have been obtained when using recent CMB data [50–52].

B. Disformal case

We now discuss the constraints on the purely disformal coupled case, in which DM and dark energy are interacting via a constant disformal coupling as defined in Eq. (19) with $C(\phi) = 1$. From our choice of data sets, we deduce that a nonzero constant disformal coupling is preferred above a 2σ confidence level. When using the $H(z)+\mathrm{BAO}+\mathrm{SNIa}$ data, we observe that $D_M > 0.070$ meV^{-1} (95.4% C.L.), and when combining these data with the BBN prior, we get that $D_M > 0.074$ meV^{-1} (95.4% C.L.). The obtained limits are given in Table II. This nonzero coupling preference distinguishes the purely disformal coupling from the purely conformal coupling, although we should remark that a nonzero conformal coupling was also found to be slightly favored particularly when combining astrophysical data sets [50–52]. In the purely

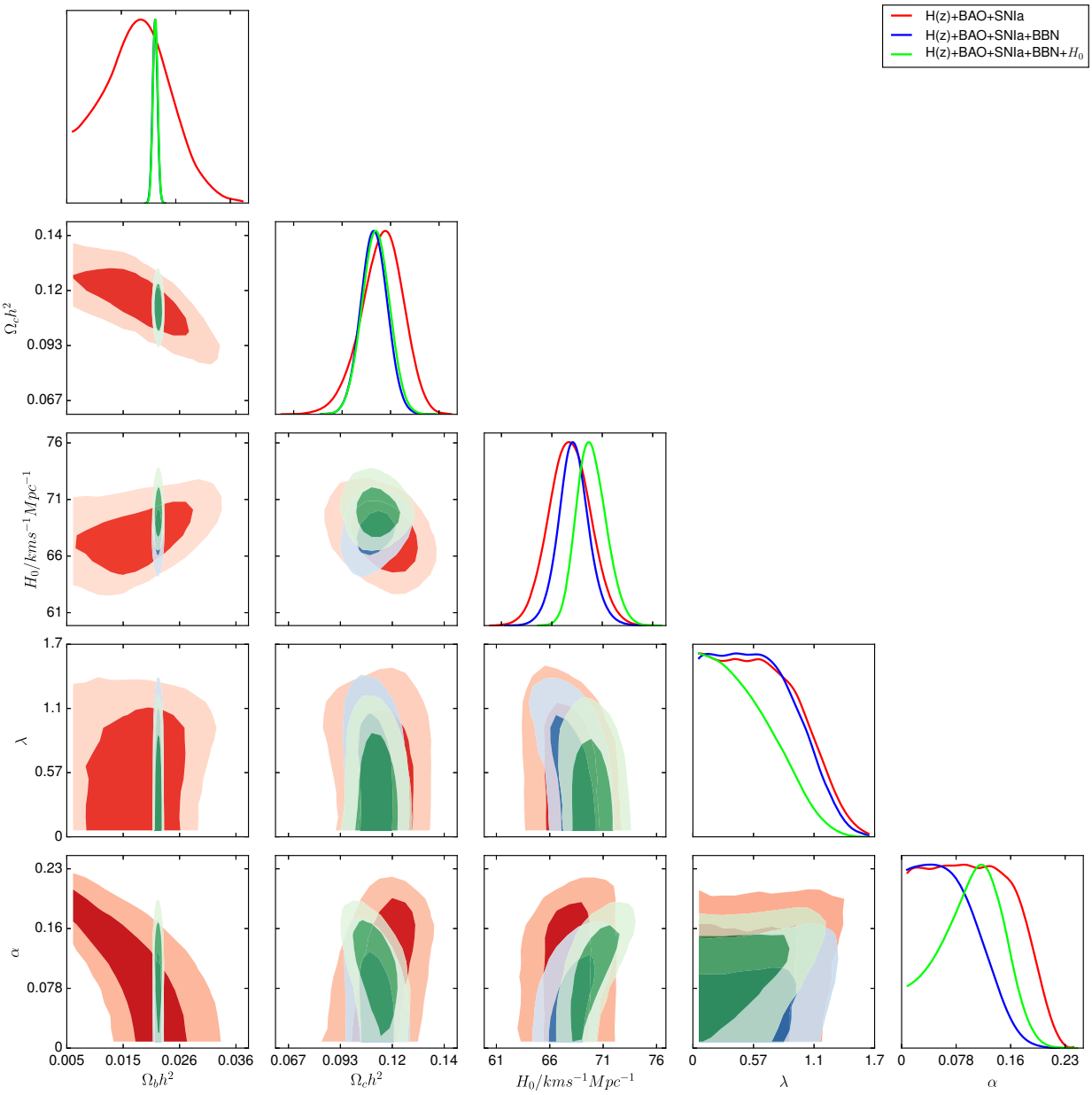

FIG. 3. Confidence-level contours of the cosmological and model parameters for the conformally coupled DM case. We compare the 68.3% (dark shaded) and 95.4% (light shaded) constraints arising from $H(z) + \text{BAO} + \text{SNIa}$ observations with $H(z) + \text{BAO} + \text{SNIa} + \text{BBN}$ and $H(z) + \text{BAO} + \text{SNIa} + \text{BBN} + H_0$ observations. The marginalized one-dimensional posterior distributions are also shown for comparison.

TABLE II. For each cosmological parameter, we report the best fit values and 1σ errors in the disformally coupled DM scenario. For λ and $D_M(\text{meV}^{-1})$, we quote the 95.4% limits instead. See the top of Sec. IV for the parameter priors.

Parameter	$H(z) + \text{BAO} + \text{SNIa}$	$H(z) + \text{BAO} + \text{SNIa} + \text{BBN}$	$H(z) + \text{BAO} + \text{SNIa} + \text{BBN} + H_0$
$\Omega_b h^2$	$0.021^{+0.0046}_{-0.0053}$	$0.022^{+0.0005}_{-0.0005}$	$0.022^{+0.0005}_{-0.0005}$
$\Omega_c h^2$	$0.11^{+0.013}_{-0.011}$	$0.11^{+0.008}_{-0.008}$	$0.11^{+0.007}_{-0.008}$
H_0	$67.57^{+2.19}_{-2.24}$	$67.79^{+1.22}_{-1.11}$	$68.53^{+0.95}_{-0.92}$
λ	<1.56	<1.56	<1.53
D_M	>0.070	>0.074	>0.094

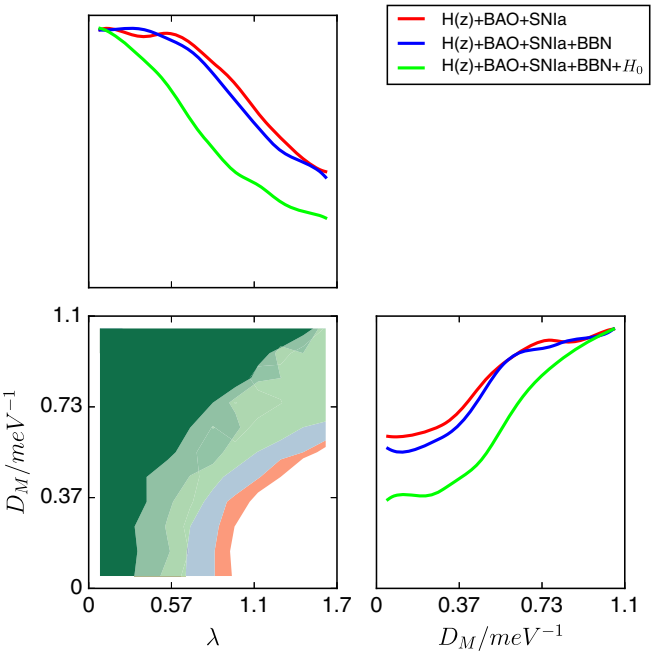

FIG. 4. Confidence-level contours of model parameters for the disformally coupled DM case. We compare the 68.3% (dark shaded) and 95.4% (light shaded) constraints arising from $H(z)+\mathrm{BAO}+\mathrm{SNIa}$ observations with $H(z)+\mathrm{BAO}+\mathrm{SNIa}+\mathrm{BBN}$ and $H(z)+\mathrm{BAO}+\mathrm{SNIa}+\mathrm{BBN}+H_0$ observations. The marginalized one-dimensional posterior distributions are also shown for comparison.

conformal case, the peak away from zero, which we discussed in Sec. IV A and which was also reported in Ref. [50–52], is still not pronounced enough to claim evidence for a deviation away from the concordance model has been found. This is due to a number of possible systematics. Moreover, larger values of the scalar field potential slope λ are allowed in comparison with the purely conformal case.

On the other hand, although the obtained limits on the disformal coupling might be tightened further by including higher-redshift experiments, our chosen data sets indicate a preference toward a nonzero disformal coupling. In such models, we find that, for a fixed potential slope λ, a weak disformal coupling [$D_M < \mathcal{O}(\mathrm{meV}^{-1})$] pushes the late-time effective equation of state to w_ϕ or larger, i.e. $\gtrsim -1$, whereas larger disformal couplings [$D_M \sim \mathcal{O}(\mathrm{meV}^{-1})$] are found to decrease the effective equation of state in the late-time Universe. Such behavior is depicted in the top right panel of Fig. 1.

Despite the fact that different probes were used, in Refs. [76,77] for example, it was found that, due to the tension between different H_0 measurements, dynamical dark energy models with a time-dependent equation of state that cross the phantom boundary into superacceleration are favored by about 2σ.

When we further include the H_0 prior with the other data sets, we obtain a larger disformal coupling lower limit of $D_M > 0.094\ \mathrm{meV}^{-1}$ (95.4% C.L.). This is similar to what happened in the purely conformal case; i.e. we can tentatively say that the H_0 prior favors an interacting dark sector irrespective of the functional form of the dark sector coupling. The confidence-level contours and the corresponding one-dimensional posterior distributions of the model parameters are shown in Fig. 4.

C. Mixed conformal disformal case

We now allow for both conformal and disformal couplings between dark matter and dark energy. As to be expected, the obtained constraints on parameters are weaker than those obtained in the purely conformal and the purely disformal cases presented above. We compare the results from different runs in Table III. The obtained upper limit on the conformal coupling parameter is given by $\alpha < 0.453$ (95.4% C.L.) when using the $H(z)+\mathrm{BAO}+\mathrm{SNIa}$ data sets and also when including the BBN prior. When we further include the H_0 prior, the full range of our chosen prior is allowed, i.e. $\alpha < 0.480$ (95.4% C.L.). Hence, in the presence of an additional disformal coupling, larger conformal couplings are allowed. In this mixed model, the lower limits on the constant disformal coupling are given by $D_M > 0.102\ \mathrm{meV}^{-1}$ (95.4% C.L.) when using the $H(z)+\mathrm{BAO}+\mathrm{SNIa}$ data sets, $D_M > 0.143\ \mathrm{meV}^{-1}$ (95.4% C.L.) when including the BBN prior, and $D_M > 0.105\ \mathrm{meV}^{-1}$ (95.4% C.L.) when we further add

TABLE III. For each cosmological parameter, we report the best fit values and 1σ errors in the conformally disformally coupled DM scenario. For λ, α, and $D_M(\mathrm{meV}^{-1})$, we quote the 95.4% limits instead. See the top of Sec. IV for the parameter priors.

Parameter	$H(z)+\mathrm{BAO}+\mathrm{SNIa}$	$H(z)+\mathrm{BAO}+\mathrm{SNIa}+\mathrm{BBN}$	$H(z)+\mathrm{BAO}+\mathrm{SNIa}+\mathrm{BBN}+H_0$
$\Omega_b h^2$	$0.021^{+0.0046}_{-0.0052}$	$0.022^{+0.0005}_{-0.0005}$	$0.022^{+0.0005}_{-0.0005}$
$\Omega_c h^2$	$0.11^{+0.011}_{-0.011}$	$0.11^{+0.008}_{-0.008}$	$0.11^{+0.010}_{-0.008}$
H_0	$67.49^{+2.13}_{-2.13}$	$67.77^{+1.10}_{-1.12}$	$69.68^{+1.04}_{-1.16}$
λ	<1.59	<1.58	<1.52
α	<0.453	<0.453	<0.480
D_M	>0.102	>0.143	>0.105

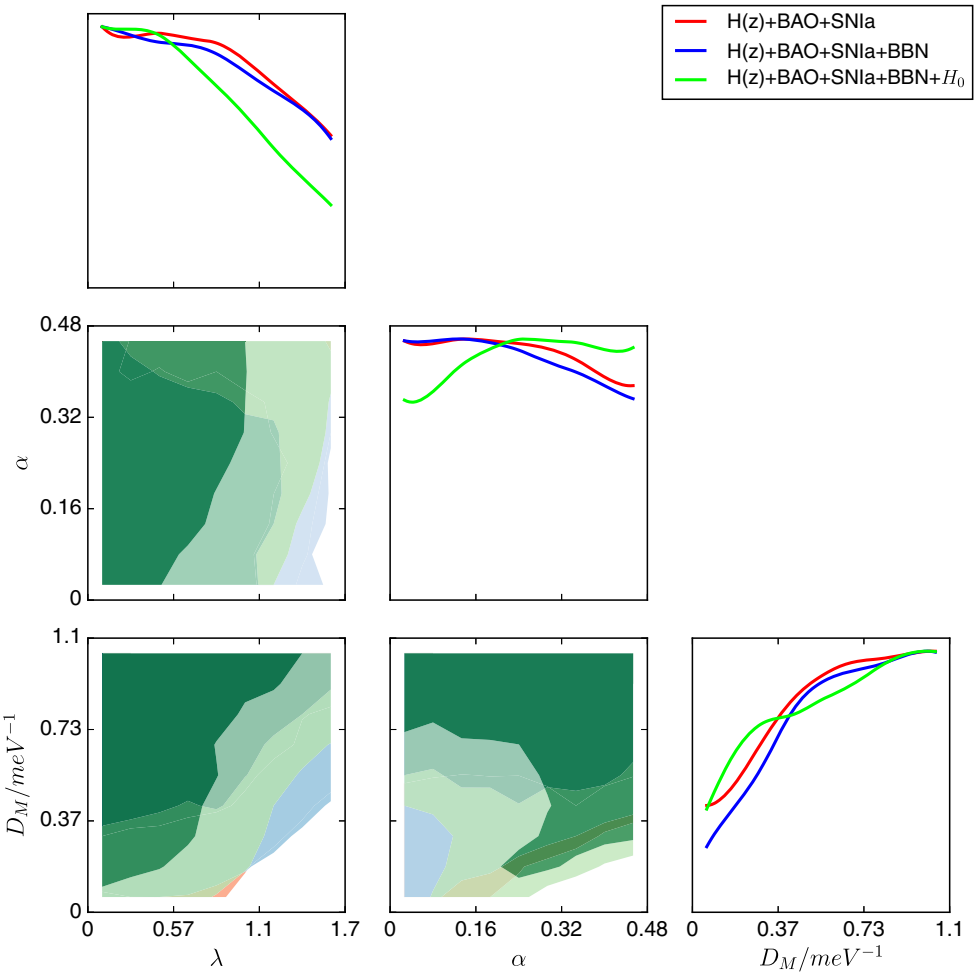

FIG. 5. Confidence-level contours of the model parameters for the conformally disformally coupled DM case. We compare the 68.3% (dark shaded) and 95.4% (light shaded) constraints arising from $H(z) + \text{BAO} + \text{SNIa}$ observations with $H(z) + \text{BAO} + \text{SNIa} + \text{BBN}$ and $H(z) + \text{BAO} + \text{SNIa} + \text{BBN} + H_0$ observations. The marginalized one-dimensional posterior distributions are also shown for comparison.

the H_0 prior. Again, a larger disformal coupling is preferred in comparison with the purely disformal case. The effective equation of state discussion presented in Sec. IV B also applies to this model. Indeed, the evolution of the effective equation of state in these models is similar to that obtained in purely disformal models. An illustration is given in Fig. 1. The confidence-level contours and the corresponding one-dimensional posterior distributions of the model parameters are shown in Fig. 5. The obtained contours are much wider than those obtained in the previous models, although high-redshift probes might shrink these contours and provide better best fits on parameters.

V. CONCLUSIONS

In the present work, we have considered an interacting dark sector in which we allowed for two distinct forms of couplings that connect dark matter with dark energy, where the latter is responsible for the cosmological acceleration. Our current state of ignorance regarding the physics of this dark sector still allows for other interactions beyond the purely gravitational ones to exist between its elements. Various dark sector models involving various coupling functions have been extensively studied, together with their astrophysical and cosmological consequences, and it is these studies, that compare such models with state-of-the-art cosmological data, that will allow us to separate the viable candidates from the false.

We here considered a specific coupled dark energy model in which dark energy and dark matter are allowed to couple via a conformal coupling and/or a disformal coupling. We first considered the purely conformal and the purely disformal coupling cases, and finally we also discussed the mixed scenario in which both a conformal and a disformal coupling are present. In our analyses, we have only used the cosmological background evolution to constrain cosmological model parameters, namely Hubble parameter measurements, baryon acoustic oscillation

distance measurements, and the Supernovae Type Ia Union2.1 compilation consisting of 580 data points.

In the conformally coupled model, we obtained results consistent with those found in the literature, although weaker constraints were obtained as we use only the background evolution to test the models. Allowing for an additional constant disformal coupling term, we found that the constraints on the conformal coupling are relaxed. This is consistent with the observations made in Ref. [38], in which it was shown that the disformal term suppresses the coupling Q at larger redshifts and therefore has an impact on the evolution of the effective equation of state $w_{\rm eff}$.

We also found that, with our choice of data sets, a nonzero disformal coupling between dark matter and dark energy is preferred over the ΛCDM model. In the purely conformal coupled case, only the analysis including the H_0 prior prefers a nonzero coupling at 1σ confidence level. In the case of a purely disformal coupling, a nonzero coupling is preferred in all analyses, as is the case in the conformally disformally coupled scenario. We must now go beyond the background evolution and consider the growth of perturbations as well. Using precise measurements of CMB anisotropies and the matter power spectra of large scale structures, we certainly expect to get tighter constraints on our model parameters. We address this in future work.

Finally, on a more speculative note, we can compare our findings above with that of Ref. [78], wherein Planck, SNIa, and redshift space distortion data are found to favor a late-time interaction between dark sector elements—it is shown in Ref. [38] that the disformal coupling of the type we have just considered switches on at late times and is negligible in the past. We merely highlight this curiosity now and return to a comparison between the models in future work.

ACKNOWLEDGMENTS

We would like to thank J. Lesgourgues for fruitful discussion. The work of C. v. d. B. is supported by the Lancaster-Manchester-Sheffield Consortium for Fundamental Physics under STFC Grant No. ST/L000520/1.

[1] S. Perlmutter *et al.* (Supernova Cosmology Project Collaboration), Astrophys. J. **517**, 565 (1999).
[2] A. G. Riess *et al.* (Supernova Search Team Collaboration), Astron. J. **116**, 1009 (1998).
[3] P. M. Garnavich *et al.* (Supernova Search Team Collaboration), Astrophys. J. **509**, 74 (1998).
[4] B. P. Schmidt *et al.* (Supernova Search Team Collaboration), Astrophys. J. **507**, 46 (1998).
[5] S. Perlmutter *et al.* (Supernova Cosmology Project Collaboration), Nature (London) **391**, 51 (1998).
[6] D. J. Eisenstein *et al.* (SDSS Collaboration), Astrophys. J. **633**, 560 (2005).
[7] W. J. Percival, S. Cole, D. J. Eisenstein, R. C. Nichol, J. A. Peacock, A. C. Pope, and A. S. Szalay, Mon. Not. R. Astron. Soc. **381**, 1053 (2007).
[8] W. J. Percival *et al.* (SDSS Collaboration), Mon. Not. R. Astron. Soc. **401**, 2148 (2010).
[9] D. N. Spergel *et al.* (WMAP Collaboration), Astrophys. J. Suppl. Ser. **148**, 175 (2003).
[10] D. N. Spergel *et al.* (WMAP Collaboration), Astrophys. J. Suppl. Ser. **170**, 377 (2007).
[11] C. L. Reichardt *et al.*, Astrophys. J. **694**, 1200 (2009).
[12] P. A. R. Ade *et al.* (Planck Collaboration), Astron. Astrophys. **594**, A13 (2016).
[13] A. Einstein, Sitzungsber. Preuss. Akad. Wiss. Berlin (Math. Phys.) **1917**, 142 (1917).
[14] S. Weinberg, Rev. Mod. Phys. **61**, 1 (1989).
[15] I. Zlatev, L.-M. Wang, and P. J. Steinhardt, Phys. Rev. Lett. **82**, 896 (1999).
[16] C. Wetterich, Nucl. Phys. **B302**, 668 (1988).
[17] R. D. Peccei, J. Sola, and C. Wetterich, Phys. Lett. B **195**, 183 (1987).
[18] P. J. E. Peebles and B. Ratra, Astrophys. J. **325**, L17 (1988).
[19] T. Chiba, T. Okabe, and M. Yamaguchi, Phys. Rev. D **62**, 023511 (2000).
[20] C. Armendariz-Picon, V. F. Mukhanov, and P. J. Steinhardt, Phys. Rev. Lett. **85**, 4438 (2000).
[21] R. R. Caldwell, Phys. Lett. B **545**, 23 (2002).
[22] M. C. Bento, O. Bertolami, and A. A. Sen, Phys. Rev. D **66**, 043507 (2002).
[23] C. Gao, F. Wu, X. Chen, and Y.-G. Shen, Phys. Rev. D **79**, 043511 (2009).
[24] M. Li, Phys. Lett. B **603**, 1 (2004).
[25] A. G. Cohen, D. B. Kaplan, and A. E. Nelson, Phys. Rev. Lett. **82**, 4971 (1999).
[26] C. Wetterich, Astron. Astrophys. **301**, 321 (1995).
[27] L. Amendola, Phys. Rev. D **62**, 043511 (2000).
[28] N. Wintergerst and V. Pettorino, Phys. Rev. D **82**, 103516 (2010).
[29] V. Pettorino and C. Baccigalupi, Phys. Rev. D **77**, 103003 (2008).
[30] G. Mangano, G. Miele, and V. Pettorino, Mod. Phys. Lett. A **18**, 831 (2003).
[31] L. Amendola, Phys. Rev. D **69**, 103524 (2004).
[32] T. Koivisto, Phys. Rev. D **72**, 043516 (2005).
[33] T. S. Koivisto, arXiv:0811.1957.
[34] Z.-K. Guo, N. Ohta, and S. Tsujikawa, Phys. Rev. D **76**, 023508 (2007).
[35] C. Quercellini, M. Bruni, A. Balbi, and D. Pietrobon, Phys. Rev. D **78**, 063527 (2008).

[36] M. Quartin, M. O. Calvao, S. E. Joras, R. R. R. Reis, and I. Waga, J. Cosmol. Astropart. Phys. 05 (2008) 007.
[37] J. Valiviita, R. Maartens, and E. Majerotto, Mon. Not. R. Astron. Soc. **402**, 2355 (2010).
[38] C. van de Bruck and J. Morrice, J. Cosmol. Astropart. Phys. 04 (2015) 036.
[39] R. C. Nunes, S. Pan, and E. N. Saridakis, Phys. Rev. D **94**, 023508 (2016).
[40] P. Gu, X. Wang, and X. Zhang, Phys. Rev. D **68**, 087301 (2003).
[41] R. Fardon, A. E. Nelson, and N. Weiner, J. Cosmol. Astropart. Phys. 10 (2004) 005.
[42] A. W. Brookfield, C. van de Bruck, D. F. Mota, and D. Tocchini-Valentini, Phys. Rev. D **73**, 083515 (2006); **76**, 049901 (2007).
[43] K. Ichiki and Y.-Y. Keum, J. High Energy Phys. 06 (2008) 058.
[44] C. Wetterich, Phys. Lett. B **655**, 201 (2007).
[45] L. Amendola and C. Quercellini, Phys. Rev. D **68**, 023514 (2003).
[46] J.-Q. Xia, Phys. Rev. D **80**, 103514 (2009).
[47] V. Pettorino, L. Amendola, C. Baccigalupi, and C. Quercellini, Phys. Rev. D **86**, 103507 (2012).
[48] L. Amendola, Phys. Rev. Lett. **86**, 196 (2001).
[49] R. Bean, E. E. Flanagan, I. Laszlo, and M. Trodden, Phys. Rev. D **78**, 123514 (2008).
[50] V. Pettorino, Phys. Rev. D **88**, 063519 (2013).
[51] J.-Q. Xia, J. Cosmol. Astropart. Phys. 11 (2013) 022.
[52] P. A. R. Ade *et al.* (Planck Collaboration), Astron. Astrophys. **594**, A14 (2016).
[53] L. Amendola, V. Pettorino, C. Quercellini, and A. Vollmer, Phys. Rev. D **85**, 103008 (2012).
[54] M. Zumalacárregui, T. S. Koivisto, D. F. Mota, and P. Ruiz-Lapuente, J. Cosmol. Astropart. Phys. 05 (2010) 038.
[55] M. Zumalacarregui, T. S. Koivisto, and D. F. Mota, Phys. Rev. D **87**, 083010 (2013).
[56] T. Koivisto, D. Wills, and I. Zavala, J. Cosmol. Astropart. Phys. 06 (2014) 036.
[57] J. Sakstein, J. Cosmol. Astropart. Phys. 12 (2014) 012.
[58] C. van de Bruck, J. Morrice, and S. Vu, Phys. Rev. Lett. **111**, 161302 (2013).
[59] J. Sakstein, Phys. Rev. D **91**, 024036 (2015).
[60] C. van de Bruck, J. Mifsud, and N. J. Nunes, J. Cosmol. Astropart. Phys. 12 (2015) 018.
[61] C. van de Bruck, J. Mifsud, J. P. Mimoso, and N. J. Nunes, J. Cosmol. Astropart. Phys. 11 (2016) 031.
[62] S. Das, P. S. Corasaniti, and J. Khoury, Phys. Rev. D **73**, 083509 (2006).
[63] S. Basilakos and J. Sola, Mon. Not. R. Astron. Soc. **437**, 3331 (2014).
[64] O. Farooq and B. Ratra, Astrophys. J. **766**, L7 (2013).
[65] A. J. Cuesta *et al.*, Mon. Not. R. Astron. Soc. **457**, 1770 (2016).
[66] F. Beutler, C. Blake, M. Colless, D. H. Jones, L. Staveley-Smith, L. Campbell, Q. Parker, W. Saunders, and F. Watson, Mon. Not. R. Astron. Soc. **416**, 3017 (2011).
[67] A. J. Ross, L. Samushia, C. Howlett, W. J. Percival, A. Burden, and M. Manera, Mon. Not. R. Astron. Soc. **449**, 835 (2015).
[68] N. Suzuki *et al.*, Astrophys. J. **746**, 85 (2012).
[69] R. Cooke, M. Pettini, R. A. Jorgenson, M. T. Murphy, and C. C. Steidel, Astrophys. J. **781**, 31 (2014).
[70] R. Jimenez and A. Loeb, Astrophys. J. **573**, 37 (2002).
[71] A. G. Riess, L. M. Macri, S. L. Hoffmann, D. Scolnic, S. Casertano, A. V. Filippenko, B. E. Tucker, M. J. Reid, D. O. Jones, J. M. Silverman, R. Chornock, P. Challis, W. Yuan, P. J. Brown, and R. J. Foley, Astrophys. J. **826**, 56 (2016).
[72] A. G. Riess, L. Macri, S. Casertano, H. Lampeitl, H. C. Ferguson, A. V. Filippenko, S. W. Jha, W. Li, and R. Chornock, Astrophys. J. **730**, 119 (2011); **732**, 129(E) (2011).
[73] L. Amendola, M. Gasperini, and F. Piazza, J. Cosmol. Astropart. Phys. 09 (2004) 014.
[74] D. Blas, J. Lesgourgues, and T. Tram, J. Cosmol. Astropart. Phys. 07 (2011) 034.
[75] B. Audren, J. Lesgourgues, K. Benabed, and S. Prunet, J. Cosmol. Astropart. Phys. 02 (2013) 001.
[76] D. L. Shafer and D. Huterer, Phys. Rev. D **89**, 063510 (2014).
[77] J.-Q. Xia, H. Li, and X. Zhang, Phys. Rev. D **88**, 063501 (2013).
[78] V. Salvatelli, N. Said, M. Bruni, A. Melchiorri, and D. Wands, Phys. Rev. Lett. **113**, 181301 (2014).